Electronic Supplementary Material (ESI) for Nanoscale.

Supporting Information

Carbon Nanodots as Ligand Exchange Probes in Au@C-dot Nanobeacons for Fluorescent Turn-on detection of biothiols

*Sonam Mandani, Bhagwati Sharma, Deepa Dey and Tridib K. Sarma**

Discipline of Chemistry, School of Basic Sciences, Indian Institute of Technology Indore, IET Campus-DAVV, Khandwa Road, Indore-452017, India.

Email: tridib@iiti.ac.in

Time Resolved Fluorescence Measurements:

For the time resolved studies, we used a picosecond time correlated single photon counting (TCSPC) system from Horiba Yovin (Model: Fluorocube-01-NL). The samples were excited at 375 nm using a picosecond diode laser (model: Pico Brite-375L). The repetition rate was 5 MHz. The signals were collected at magic angle (54.70^{o}) polarization using a photomultiplier tube (TBX-07C) as the detector, which has a dark count of less than 20 cps. The instrument response function of our setup is 140 ps. The data analysis was done using IBH DAS (version 6) decay analysis software. The fluorescence decay was described as a sum of exponential functions:

$$D(t) = \sum_{i=1}^{n} a_i \exp\left(\frac{-t}{\tau_i}\right)$$

Where $D(t)$ is the normalized fluorescence decay. τ_i are the fluorescence lifetimes of various fluorescent components and a_i are the normalized pre-exponential factors. The amplitude weighted lifetime is given by:

$$\langle \tau \rangle = \sum_{i=1}^{n} a_i \tau_i$$

The quality of the fit was judged by reduced Chi square (χ^2) values and the corresponding residual distribution. To obtain the best fitting in all of the cases, χ^2 was kept near to unity.

Photostability measurements of C-dots:

For photostability test, the samples were irradiated under a low pressure UV lamp (wavelength 356 nm and power 6 W) obtained from Scientific Aids and Instrument Corporation, India. PL imaging and decay of an individual C-dot was obtained using a custom-made microscope setup based on an inverted fluorescence microscope (Nikon, Eclipse Ti-U) coupled with a back-illuminated electron-multiplying charge-coupled device (EM-CCD) camera (Andor, iXon X3 897). An air-cooled argon ion laser (Melles Griot, 400-A03) was used as a source of excitation light. A collimated laser beam of 457 nm wavelength was passed through a beam expander (Holmarc, India) and a neutral density filter (Sigma Koki, Japan). The beam was then directed

toward the center of the back aperture of an oil immersion objective (Apo TIRF, Nikon, 100×, NA = 1.49) parallel to the objective axis and subsequently focused on its back focal plane. The PL signal was filtered by a 505 nm dichroic mirror and a 520 nm long-pass filter. Finally, the images were captured by the back illuminated EM-CCD camera at a frame rate of 200 ms with no binning. The images were analyzed with ImageJ (version 1.47v) by the National Institutes of Health (NIH).

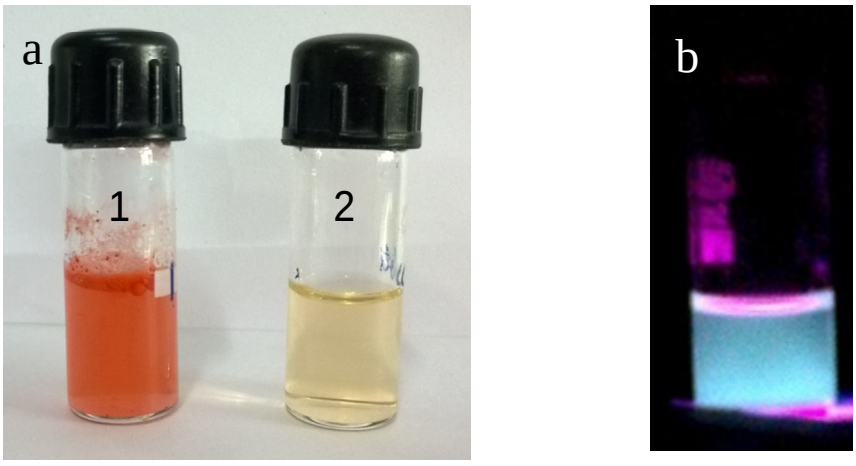

Figure S1. Digital images of (a) β-carotene dispersed in water (1) and after formation of C-dots (2). (b) C-dot solution showing blue fluorescence under UV light (λ_{ex}= 365 nm).

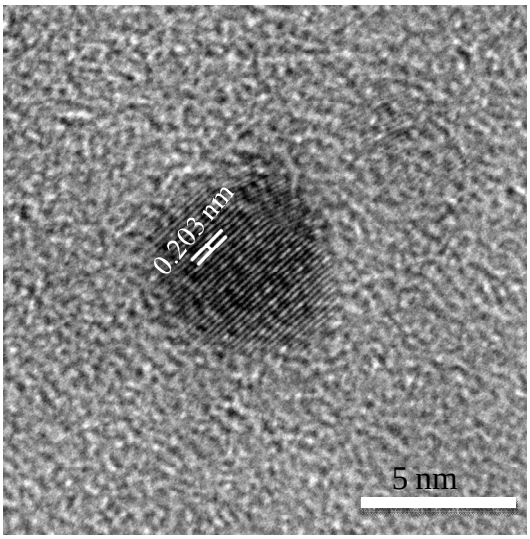

Figure S2. High resolution transmission electron microscopy image of carbon dots showing lattice separation of 0.203 nm corresponding to (102) plane of graphitic (sp^2) carbon.

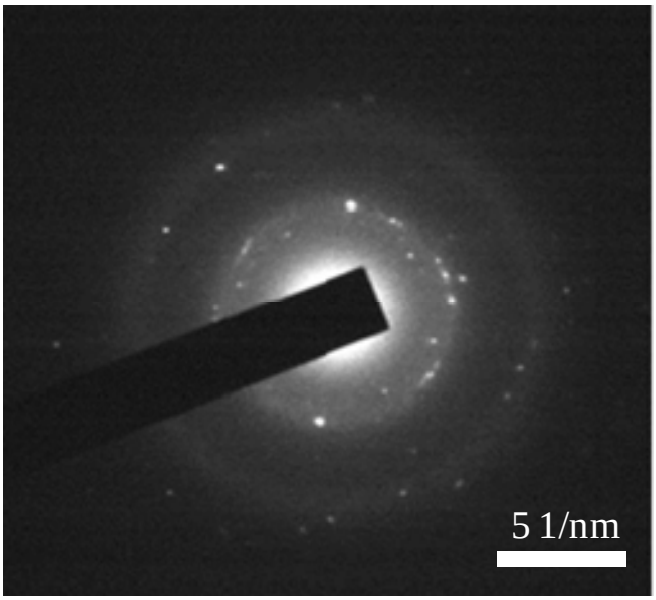

Figure S3. Selected area electron diffraction pattern (SAED) of C-dots showing its crystalline nature.

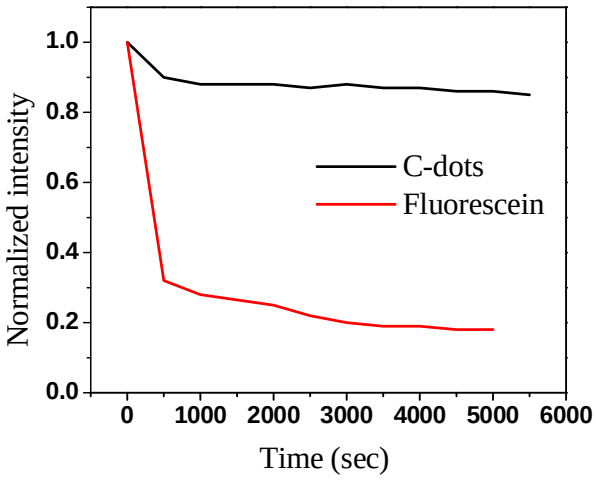

Figure S4. Photobleaching properties of C-dots and fluorescein under a UV lamp (356 nm) illumination.

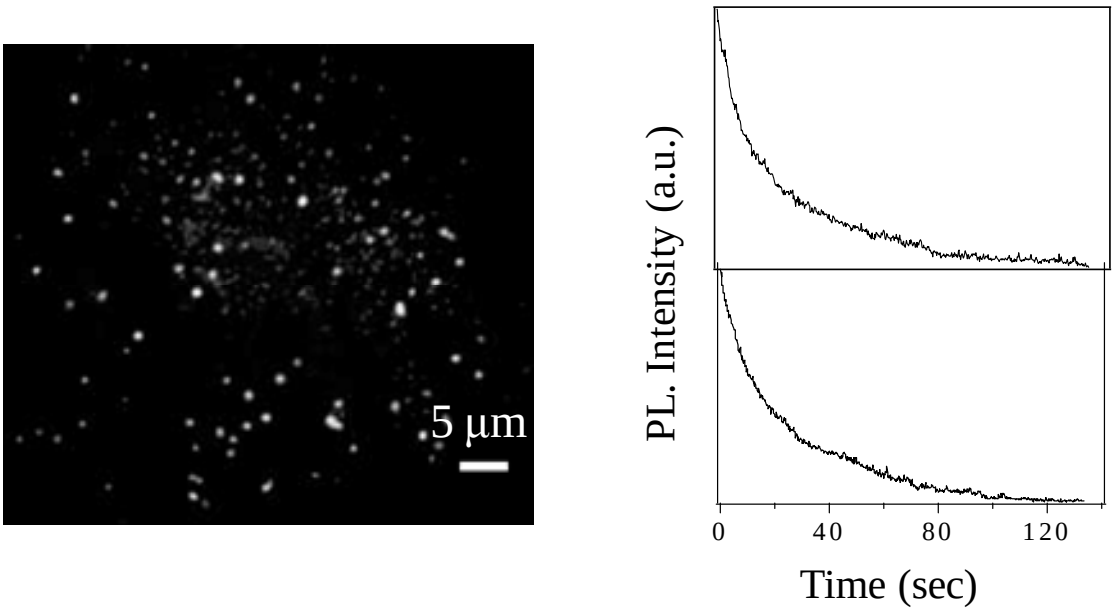

Figure S5. a) PL image of C-dots and b) PL time traces of two luminescent spots

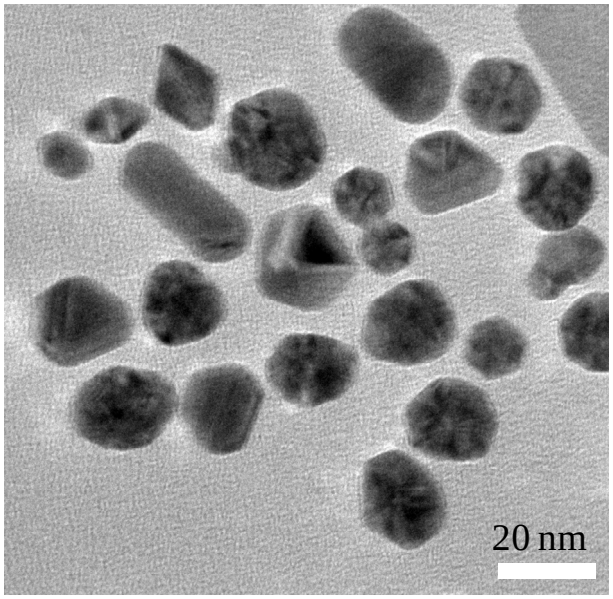

Figure S6: TEM image of Au@C-dot composite showing nanostructures of various shapes such as rods, polyhedral etc.

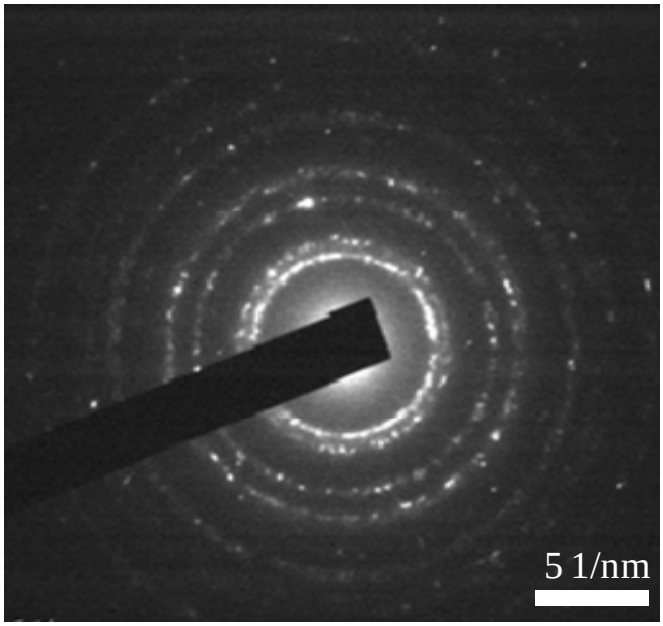

Figure S7. SAED pattern of Au NPs showing ring pattern, synthesized using carbon dots as reducing as well as stabilizing agent.

FTIR Studies:

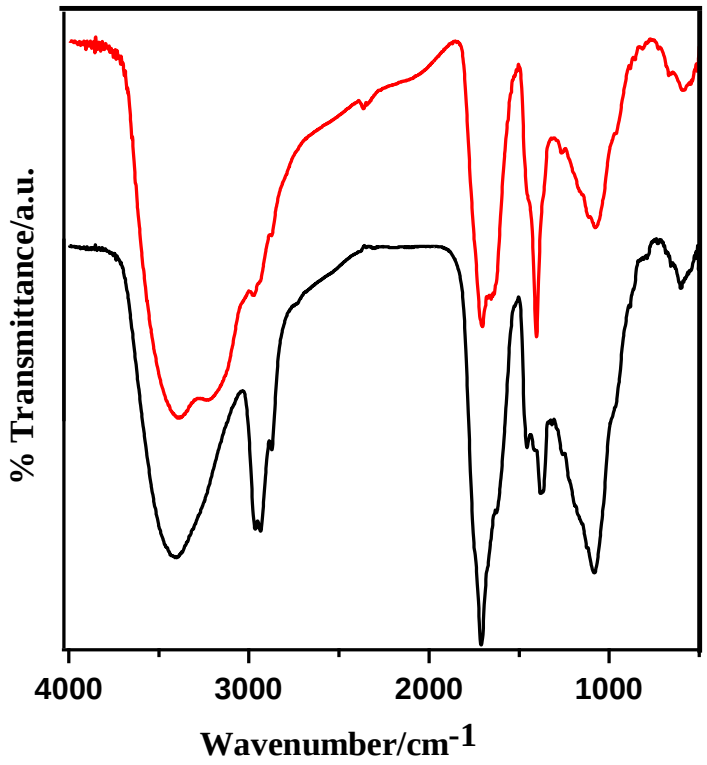

Figure S8. FTIR spectra of C-dots (black) and Au@C-dot nanocomposite (red).

C-dots, in general consist of covalently attached oxygen containing functionalities, such as hydroxyl, carboxyl and carbonyl. The FTIR spectrum of C-dots illustrate the characteristic features including stretching vibrational peak of O-H at 3400 cm^{-1}, the C=O stretching vibrational peak at 1710 $cm^{-1}$and the C-O stretching vibration at 1080 cm^{-1}. The peak at 2940 cm^{-1} can be ascribed to C-H stretching vibrations. In the Au@C-dot, it was observed that the C=O stretching peak at 1710 cm^{-1} decreased in intensity and was shifted to 1700 cm^{-1}. Also the C-O stretching frequency was shifted from 1080 cm^{-1} to 1072 cm^{-1}, indicating their possible involvement in the reduction and stabilization of the Au nanoparticles.

Raman Studies:

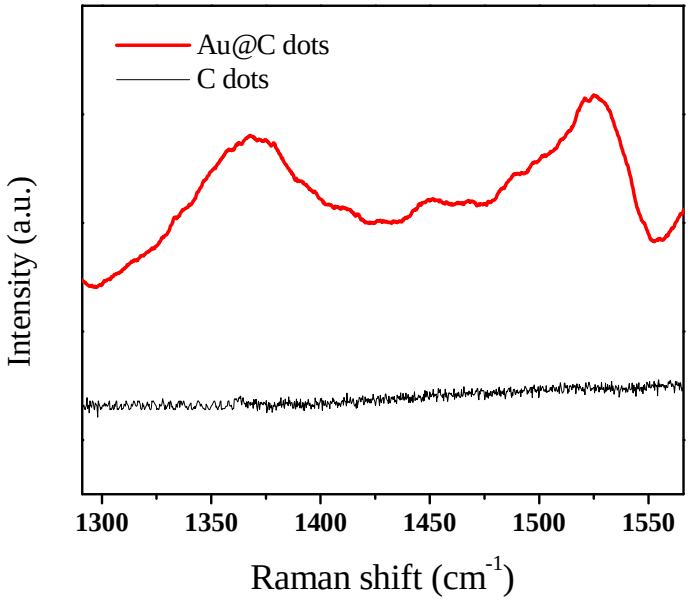

Figure S9. Typical Raman spectra of C-dots (black) and Au@C-dot composites (red).

Stability of C-dots and Au@C-dot at different solution pH:

The fluorescence intensity of both C dots and Au@C dots is pH dependent as depicted in Figure 1. It was observed that, althought the emission wavelength did not change significantly (λ_{ex}= 370 nm, λ_{em}= 470 nm), the fluorescence intensity was found to be variable with change in pH. Both C dots as well as Au@C dots showed strongest PL emission around pH 6 while the emission decreased in highly acidic or alkaline conditions.

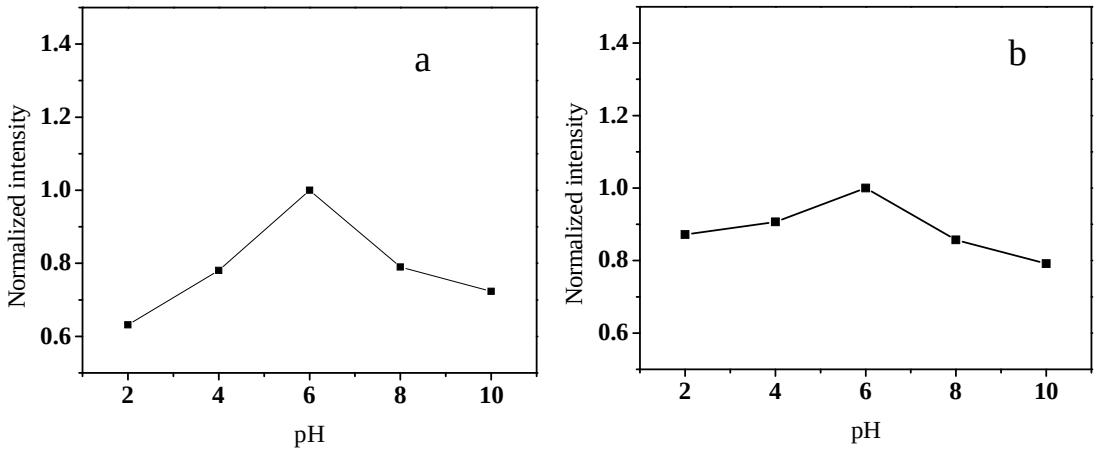

Figure S10. Variation in fluorescence intensity of (a) C dots and (b) Au@ C dots with pH.

Stability of C-dots and Au@C-dot at different ionic strength of NaCl aqueous solution:

In order to realize the stabilization of C-dots and Au@C-dot composite at different ionic strength of NaCl aqueous solution, we studied the fluorescence intensity of the two probes. The emission wavelength of C-dots and Au@C-dots were not affected with the change in ionic strength of the medium. As shown in Figure S11a, there was no obvious change in the PL intensity of C-dots even in a NaCl aqueous solution with high ionic strength (0.5 M). On the other hand, in case of Au@C-dot composite, we observed a gradual increase in the PL intensity with increasing ionic strength of the NaCl aqueous solution, as shown in Figure S11b and S11c. It was observed that the color of the Au@C-dot composite turned from pink to blue with the addition of NaCl. This was also confirmed with UV-visible spectroscopy where we observed a red-shift in the plasmon resonance band position of Au@C-dot from 528 nm to 600 nm (Figure S11d). It is a well-known fact that salt induces an irreversible agglomeration of the charge-stabilized nanoparticles reflecting a colorimetric change in the nanoparticles.

In case of Au@C-dot composite, we have observed experimentally (as discussed in the manuscript) that the fluorescence inherent to C-dots is quenched after the formation of Au NPs and the quenching mechanism was found to be a combination of static as well as dynamic quenching. The dynamic quenching is through the Förster resonance energy transfer (FRET) mechanism, where the energy transfer between the donor and acceptor depends on the overlap of emission spectra of C-dots and absorption spectra of Au NPs. In case of Au@C-dot composite,

there was significant overlap between the emission spectra of C-dots and the plasmon resonance band of Au nanoparticles. On the other hand, the particles get aggregated in the presence of NaCl and the plasmon resonance band shifted to a longer wavelength. Hence the spectral overlap of the emission inherent to C-dots and plasmon resonance band of the agglomerated Au@C-dot becomes less significant. We believe that the enhancement of PL intensity of Au@C-dot with increase in ionic strength of NaCl aqueous solution due to the inefficient FRET as the spectral overlap minimizes. It is worth mentioning that this enhancement in the PL intensity is not much significant compared to the enhancement in PL intensity when a biothiol was added leading to surface modification of Au nanoparticles and release of C-dots.

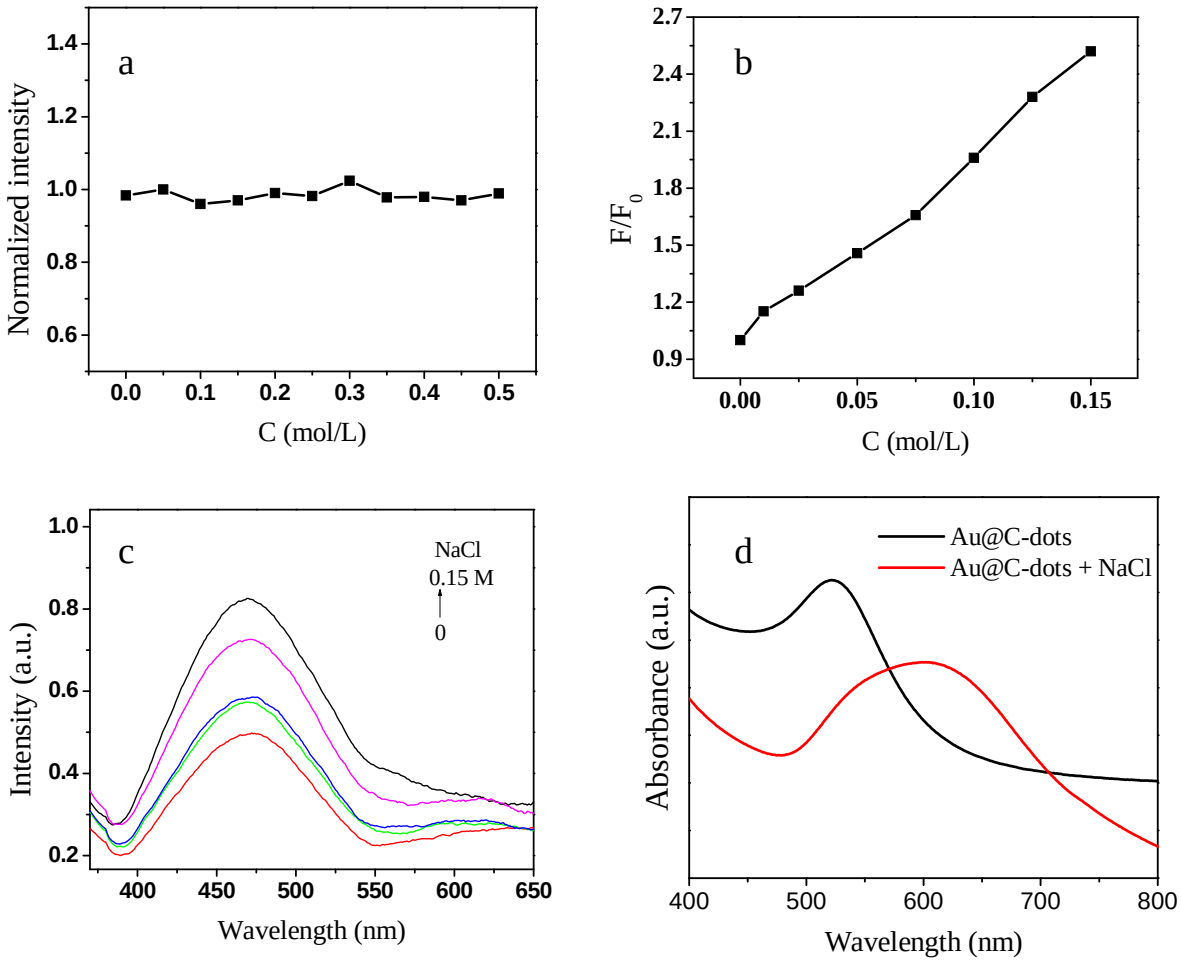

Figure S11. The effect of different ionic strength of NaCl aqueous solution on the fluorescence intensity of (a) C-dots (b) Au@C-dot composite; the fluorescent spectra of Au@C-dot composite with increasing ionic strength of NaCl aqueous solution (c) ; UV-visible spectra of Au@C-dot and Au@C-dot in a 0.2 M NaCl aqueous solution(d).

Effect of temperature:

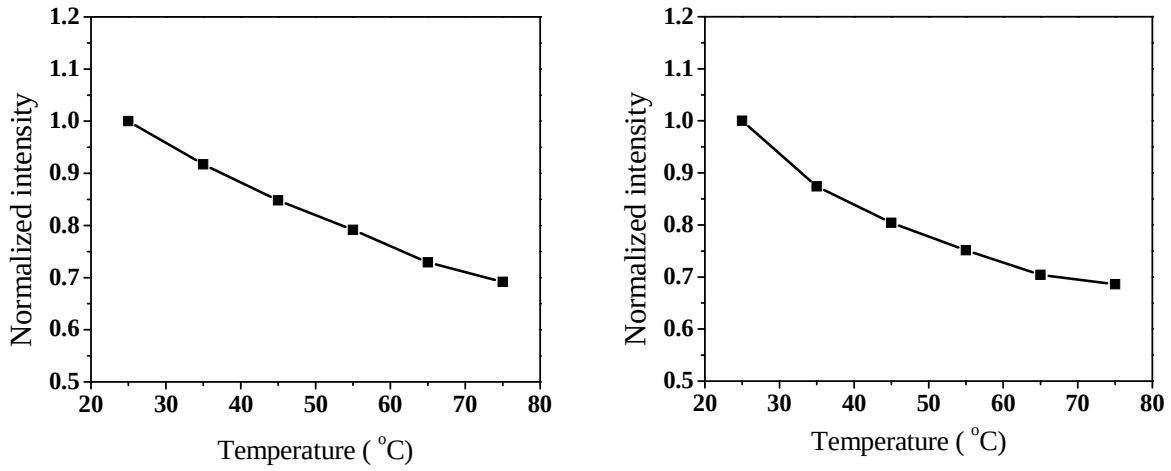

Figure S12. Variation in fluorescence intensity of (a) C-dots (b) Au@C-dots at various temperature.

As shown in Figure 3, the fluorescence intensity of both C-dots and Au@C-dots decreased with increase in temperature (PL intensity loss at 75°C = 31% in case of C-dots and 33% in case of Au@C-dot). This could be attributed to the nonradiative relaxation originated from the thermal activation of nonradiative trappings. A detailed mechanistic investigation towards temperature dependence of C-dots has been studied in great details by Yu et. al.[1]

Table S1. Fluorescence lifetime of as synthesized C-dots, Au@C-dots and recovered C-Dots excited at 375 nm.

Samples	a_1	a_2	a_3	τ_1 (ns)	τ_2 (ns)	τ_3 (ns)	τ_{av} (ns)	χ^2
Synthesized CDs	0.71	0.29	0	0.943	4.28	0	1.910	1.29
Au@CD	0.27	0.13	0.60	1.214	4.291	0.199	1.003	1.16
Recovered CDs	0.70	0.30	0	0.876	3.98	0	1.807	1.41

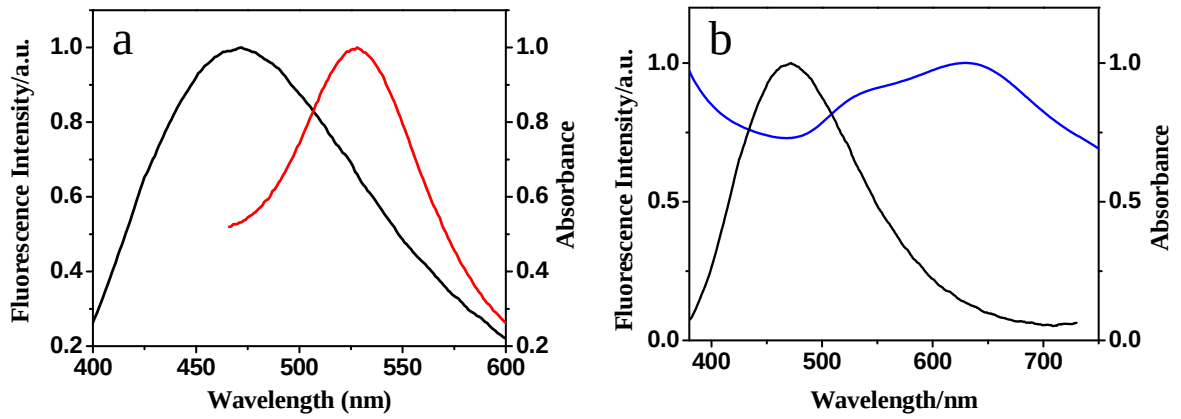

Figure S13. Spectral overlap of fluorescence emission of C-dots (black) and absorption spectra of (a) Au@C-dots (red) and (b) Au@C-dot after addition of cysteine (blue).

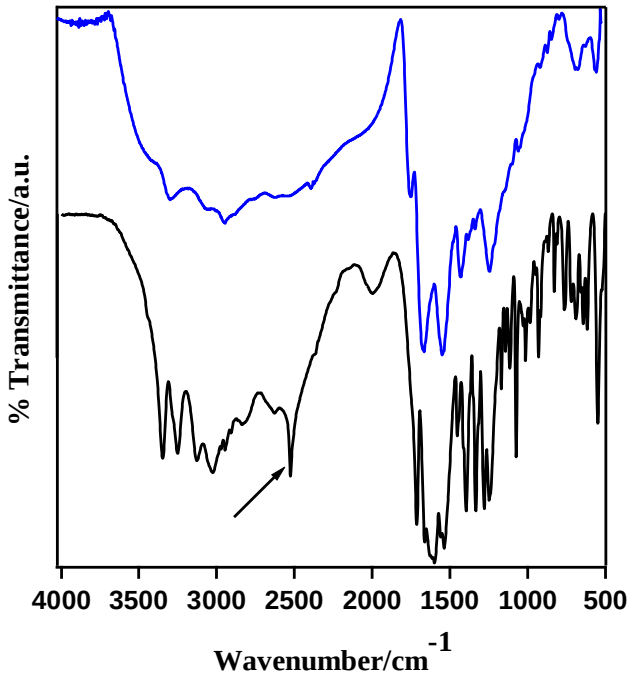

Figure S14. FTIR spectra of cysteine (black) and Au@C-dot composite (blue) after addition of cysteine. Arrow in black indicates –SH stretching at 2526 cm^{-1} which is absent in the nanocomposite.

TCSPC Studies:

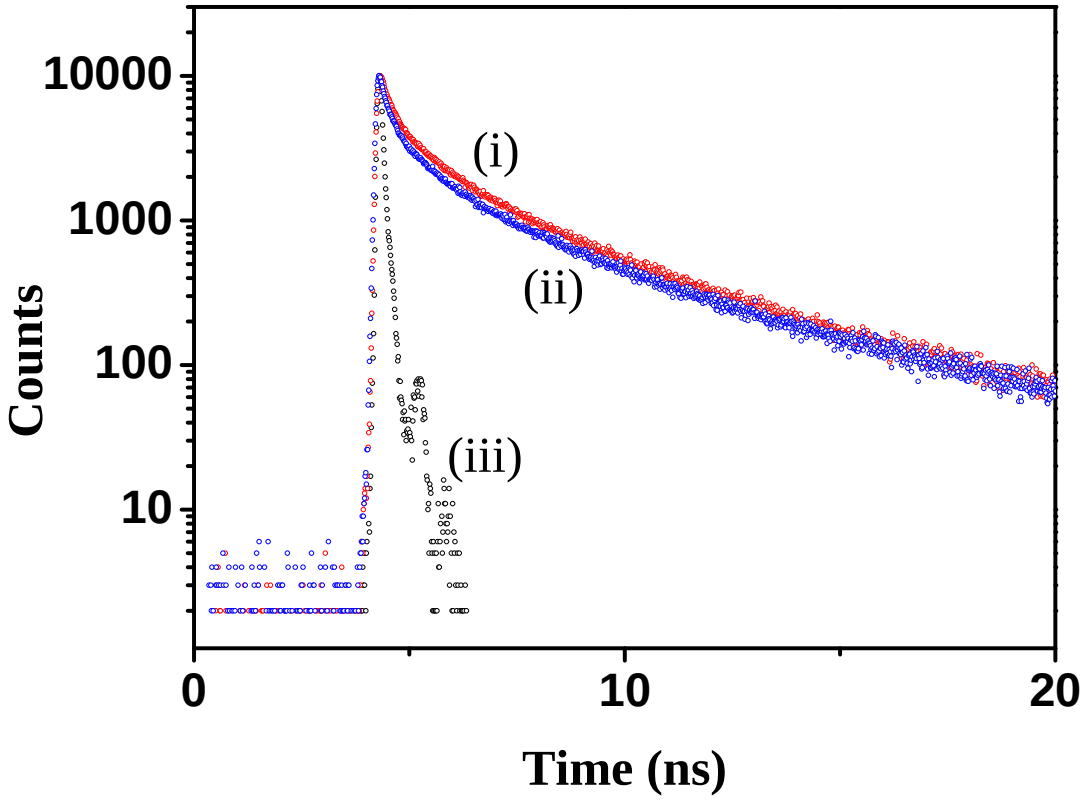

Figure S15. Lifetime decay curves of (i) synthesized carbon dots, (ii) carbon dots recovered after precipitating Au nanoparticles from Au@C-dots after addition of cysteine and (iii) is the instrument response function.

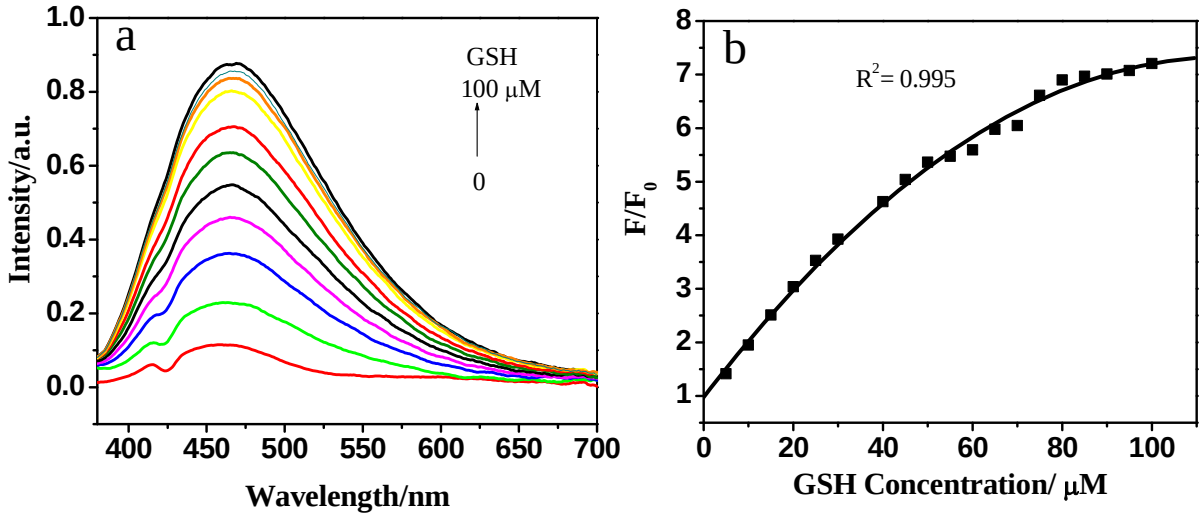

Figure S16. (a) Fluorescence spectrum of Au@C-dot after addition of increasing concentrations of glutathione and (b) Relative fluorescence (F/F_0) of Au@C-dots as a function of glutathione concentration.

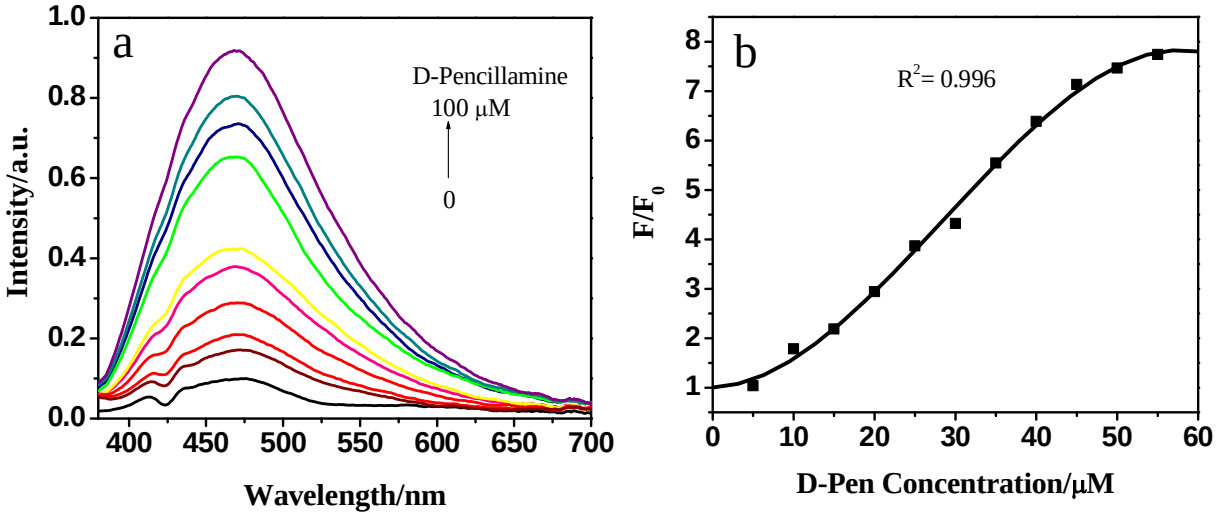

Figure S17. (a) Fluorescence spectrum of Au@C-dots after addition of increasing concentrations of D-Penicillamine and (b) Relative fluorescence (F/F_0) of Au@C-dots as a function of D-Penicillamine concentration.

Table S2. No. of cysteine residues in different proteins.[2-5]

Proteins	Number of cysteine residues
Bovine Serum Albumin	18
Urease	27-35
Pepsin	7
Glucose Oxidase	2

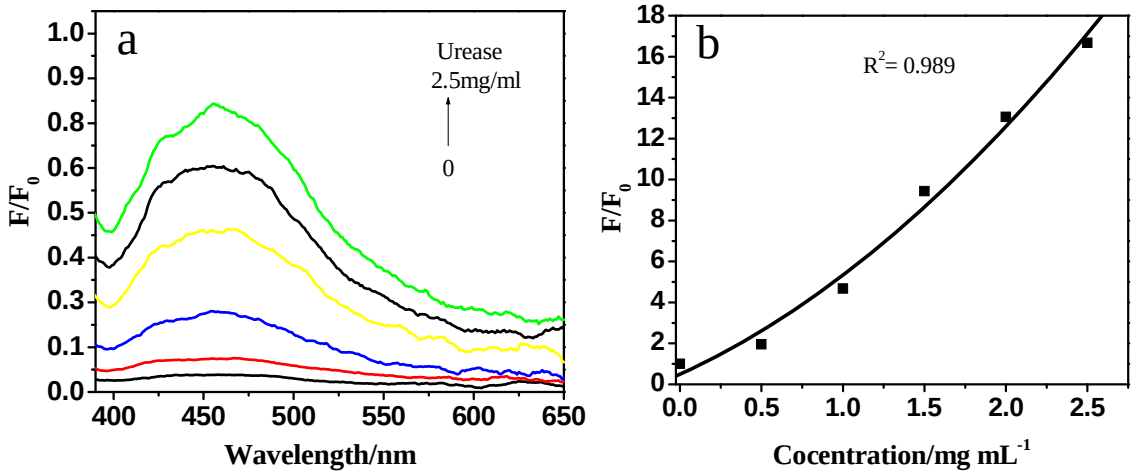

Figure S18. (a) Fluorescence spectrum of Au@C-dot after addition of increasing concentrations of urease and (b) Relative fluorescence (F/F_0) of Au@C-dots as a function of urease concentration.

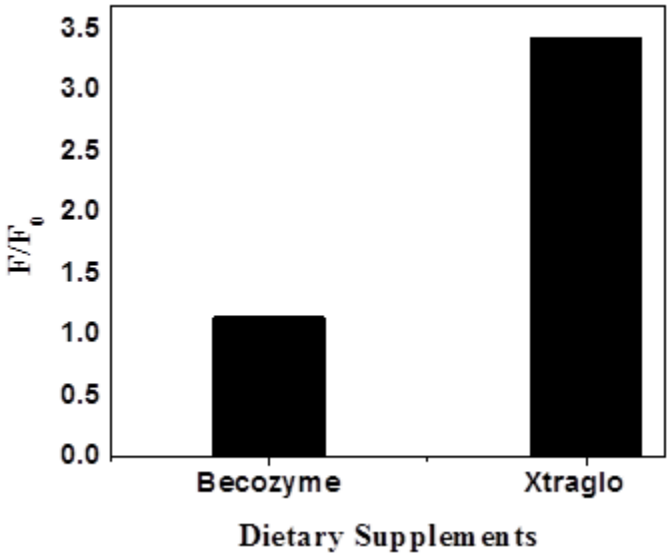

Figure S19. Relative fluorescence (F/F_0) of Au@C-dots as a function of dietary supplement tablets.

References

1. P. Yu, X. Wen, Y. – R. Toh, J. Tang , *J. Phys. Chem. C*, 2012, 116 (**48**), 25552–25557.
2. Y. Xu, J. Sherwood, Y. Qin, D. Crowley, M. Bonizzonic, Y. Bao, *Nanoscale* 2014, **6**, 1515-1524.
3. K. Takishima, T. Suga, G. Mamiya, *Eur. J. Biochem.* 1988, **175**, 151-165.
4. H. Kawasaki, K. Hamaguchi, I. Osaka, R. Arakawa, *Adv. Funct. Mater.* 2011, **21**, 3508.
5. H. Tsuge, O. Natsuaki, K. Ohashi, *J. Biochem*. 1975, **78**, 835-843.